

Lecture 4

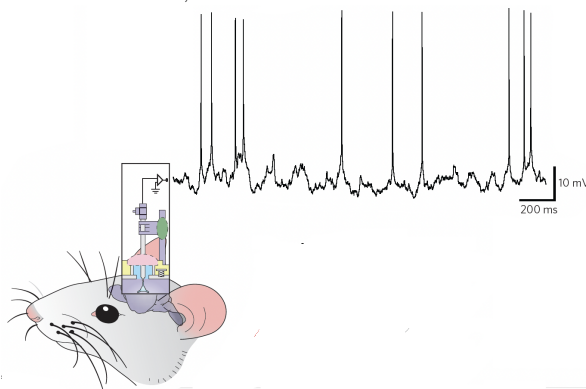
Revised 13 January 2022 00:20

## 4 Recording and activation of neurons

### 4.1 Modern twists on classical techniques

Classical intracellular recording makes use of glass cylindrical electrodes that provide an intracellular connection to a cell. The modern twist is intracellular recording from a cortical or hippocampal neurons in a mouse that is running on a maze (Figure 1). This shows, for example, that neurons can have so much excitatory drive at the center of their receptive field that the cell is essentially shunted (Figure 2); this phenomena would be missed by extracellular electrodes.

Figure 1: Head-mount for jerk-free insertion of an electrode into a pyramidal cell. From Lee, Manns, Sakmann and Brecht, 2006



Classical extracellular recording makes use of metal electrodes that record the flow of current outside of a cell and provide a means to infer spikes in a neighboring cell. The modern twist is extracellular recording from hundreds of sites at once (Figure 3).

### 4.2 Genetically expressed optical-based indicators of intracellular $Ca^{2+}$

In a program started by the late Roger Tsien, these molecules (Figure 4.2) are expressed in vivo in specific cell types and initiate an increase in fluorescence in response to the  $Ca^{2+}$  influx that follows an action potential (Figure 5).

Figure 2: Recording from neurons in CA1 of hippocampus as the mouse passes through its place field; bursts of spikes occurred at regions marked by red dots. From Epsztein, Brecht and Lee, 2011

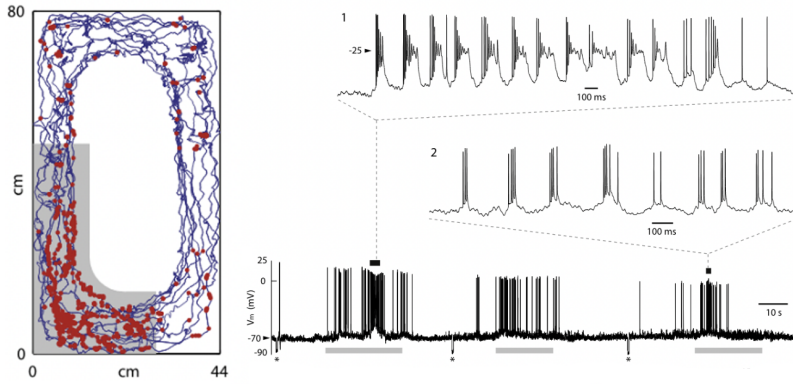
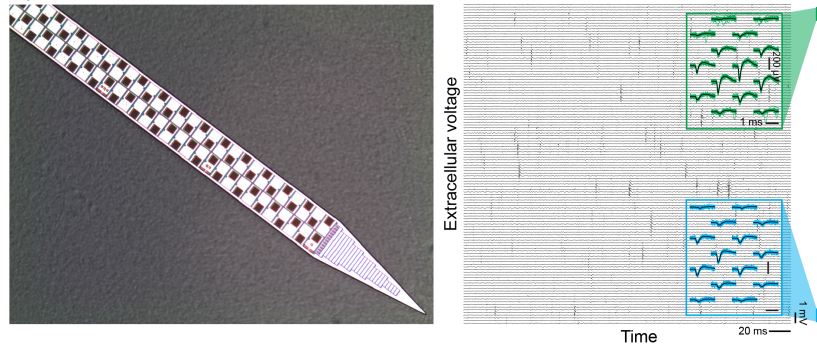


Figure 3: Recording from cortex with Neuropixels. From Jun, Steinmetz, Siegle, Denman, Bauza, Barbarits, Lee, Anastassiou, Andrei, Aydön, Barbic, Blanche, Bonin, Couto, Dutta, Gratiy, Gutnisky, Hausser, Karsh, Ledochowitsch, Lopez, Mitelut, Musa, Okun, Pachitariu, Putzeys, Rich, Rossant, Sun, Svoboda, Carandini, Harris, Koch, OKeefe and Harris, 2017



### 4.3 In vivo recording of neuronal structure and function with two-photon laser scanning microscopy

Winfried Denk's technique of two-photon laser scanning microscopy, properly pushed to the limit with corrections for the wavefront distortion through tissue (Figure 6), allows changes in intracellular  $Ca^{2+}$  to be measured in neuronal soma down to spines in nearly all layers of cortex. Note that the region of observation, the point spread function, is elongated in "z" (Figure 7).

Figure 4: The cyclically permutable GFP turned into a detector of intracellular  $Ca^{2+}$ . From Chen, Wardill, Sun, Pulver, Renninger, Baohan, Schreiter, Kerr, Orger, Jayaraman, Loofer, Svoboda and Kim, 2013.

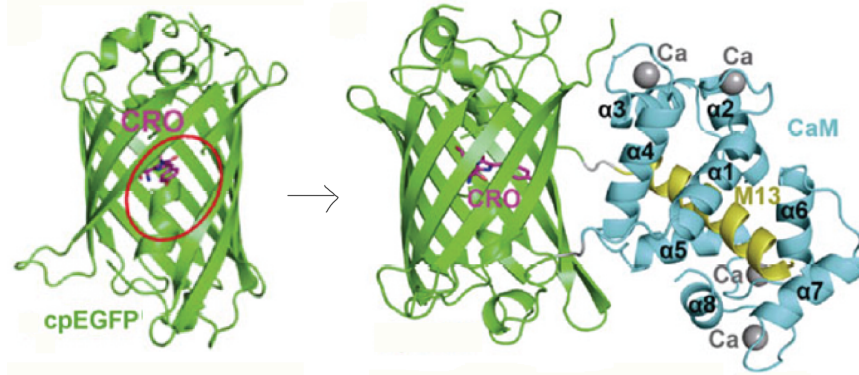
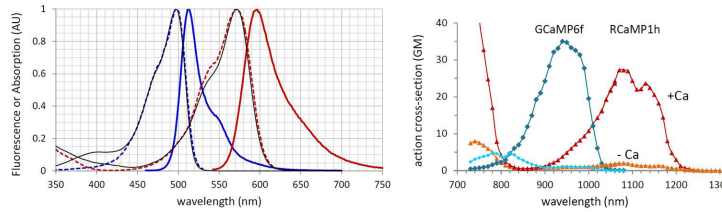


Figure 5: Absorption and fluorescent spectrum.



#### 4.4 In vivo recording of calcium signaling with two-photon laser scanning microscopy

In vivo  $Ca^{2+}$  signals may be recorded after a single spike, and from many sites (Figure 8). Still the interpretation in terms of numbers of spikes is imperfect and thus curation is suggested in quantitative interpretation of signals (Figures 4.4, 10, and 11).

#### 4.5 In vivo recording of activity in the locomoting animal

The use of virtual reality in combination with two-photon microscopy permits behavior and circuit dynamics to be concurrently measured (Figures 12 and 13).

#### 4.6 Genetically expressed optical-based drivers of spiking

Optical activation of certain microbial opsin expressed in the membrane of neurons (Figure 14), most famously channelrhodopsin (Figure 15), can be used to photo-excite, or photo-inhibit, neurons.

Figure 6: Essential components of a state-of-the-art two photon microscope. From Liu, Li, Marvin and Kleinfeld 2019.

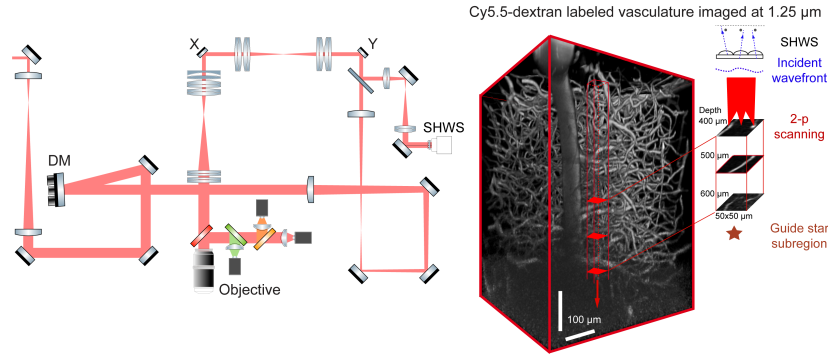
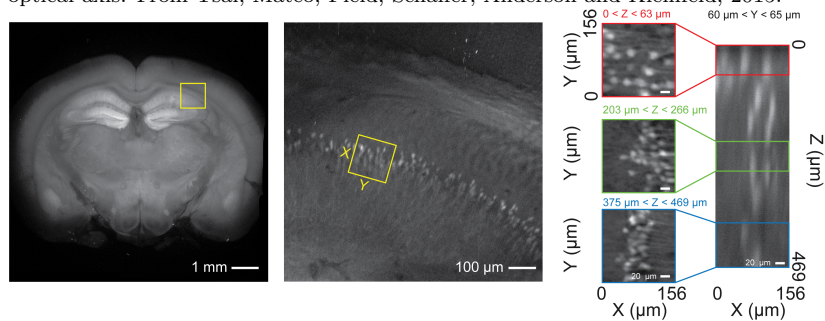


Figure 7: The distortion of cell images by the point spread function is most severe along the optical axis. From Tsai, Mateo, Field, Schaffer, Anderson and Kleinfeld, 2015.



## 4.7 All optical schemes for feedback control of spiking

The use of two-photon imaging and concurrent two-photon photoactivation permits behavior and circuit dynamics to be concurrently measured and perturbed solely with light and light-activated molecules (Figures 16, 17, 18, 19, and 20).



Figure 8: Intracellular responses in superficial V1 of mouse visual cortex using GCaMP6. From Chen, Wardill, Sun, Pulver, Renninger, Baohan, Schreiter, Kerr, Orger, Jayaraman, Loofer, Svoboda and Kim, 2019.

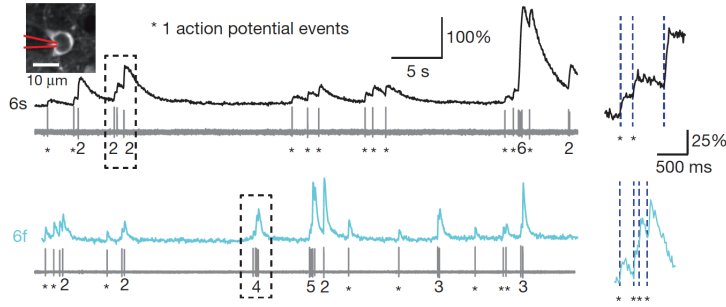


Figure 9: Intracellular responses in hippocampal brain slice with cell culture using Oregon Green BABTA. From Sasaki, Takahashi, Matsuki and Ikegaya, 2008.

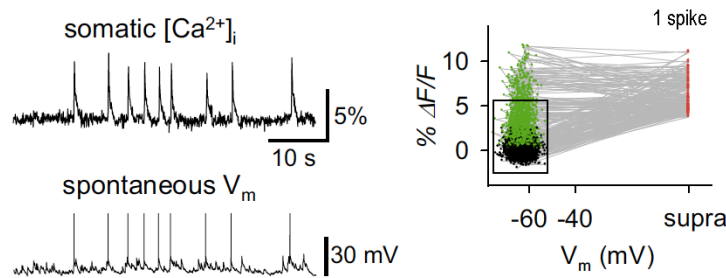


Figure 10: Intracellular  $Ca^{2+}$  is an unreliable measure of spike count and may fail to detect single spikes in vivo. From Theis, Berens, Froudarakis, Reimer, Roson, Baden, Euler, Tolias and Bethge 2016.

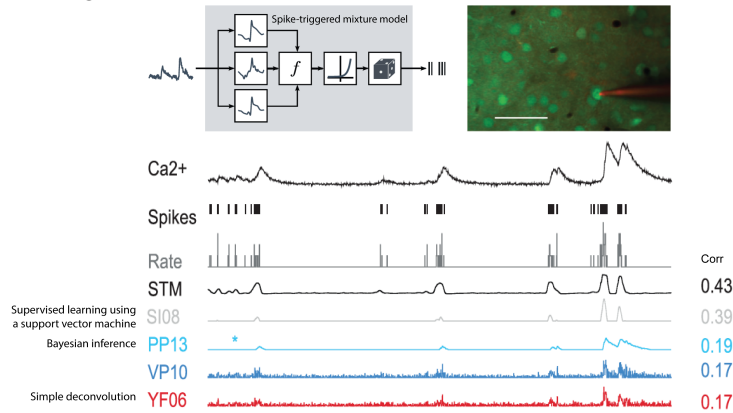


Figure 11: Intracellular  $Ca^{2+}$  in distal dendrites of L5b neurons can dissociate from somatic electrical activity. From Helmchen and Waters 2002.

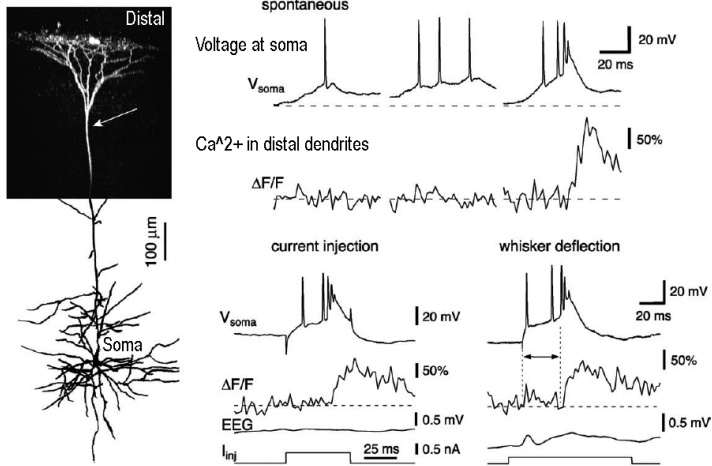


Figure 12: In vivo hippocampus preparation. From Dombeck, Harvey, Tian, Looger and Tank 2010.

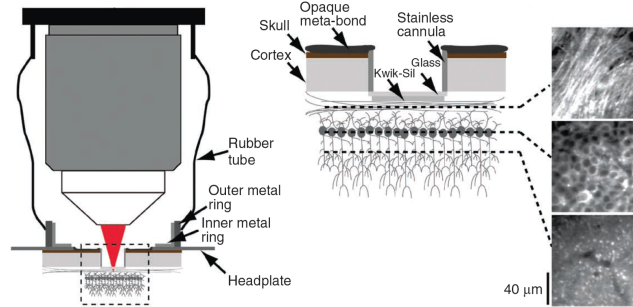


Figure 13: In vivo recording in hippocampus. From Dombeck, Harvey, Tian, Looger and Tank 2010.

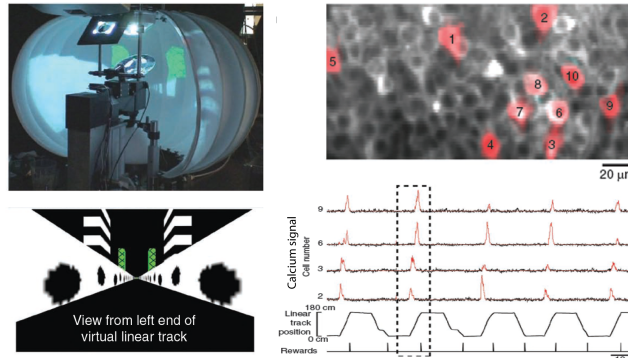


Figure 14: Natural transmembrane proteins that use light to pump ion of open ion selective pores.

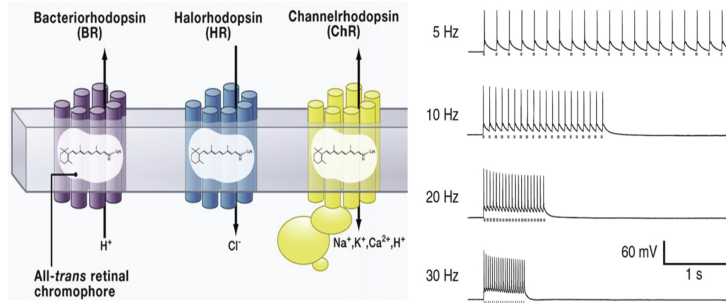


Figure 15: One photon absorption and dynamics of channelrhodopsin. From Klapoetke, Murata, Kim, Pulver, Birdsey-Benson, Cho, Morimoto, Chuong, Carpenter, Tian, Wang, Xie, Yan, Zhang, Chow, Surek, Melkonian, Jayaraman, Constantine-Paton, Wong and Boyden, 2014

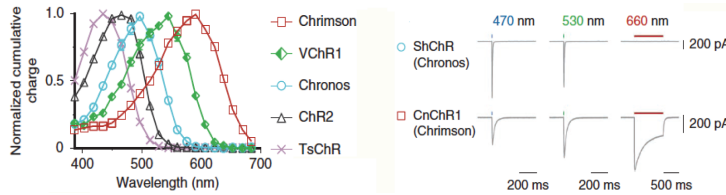


Figure 16: Two-photon action spectra for activating neurons with red-shifted channelrhodopsin C1V1 and action spectrum for recording Ca<sup>2+</sup> transients with GCaMP3.

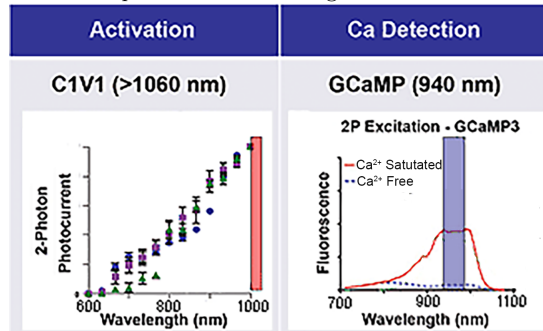


Figure 17: Narrow range of excitation for two-photon activation with red-shifted channelrhodopsin ReaChR. From Chaigneau, onzitti, Gajowa, Soler-Llavina, Tanese, Breureau, Papagiakoumou, Zeng and Emiliani, 2016

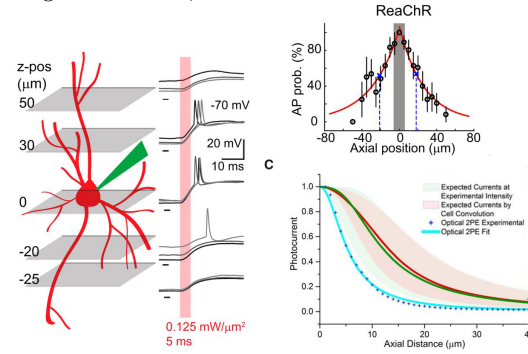


Figure 18: Schematic for feedback induced long-term synaptic potentiation. From Zhang, Russell, Packer, Gauld and Hausser 2018.

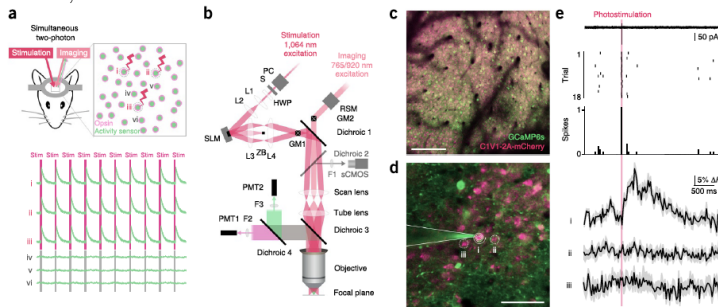


Figure 19: Test of feedback induced long-term synaptic potentiation. From Zhang, Russell, Packer, Gauld and Hausser 2018.

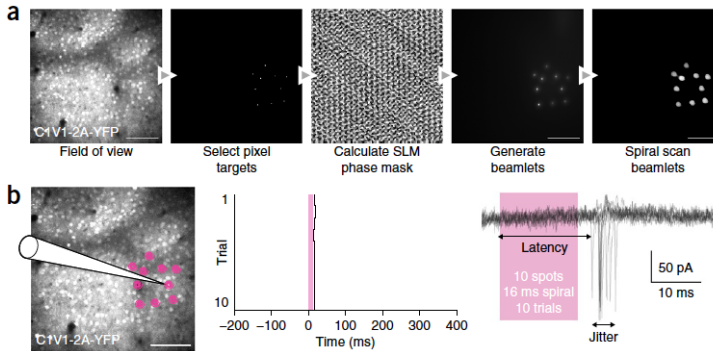


Figure 20: Test of feedback induced long-term synaptic potentiation. From Zhang, Russell, Packer, Gauld and Hausser 2018.

